

Combining Registration and Abnormality Detection in Mammography

Mohamed Hachama, Agnès Desolneux, and Frédéric Richard

MAP5, University Paris 5,
45, rue des Saints Pères,
75006 Paris, France

{hachama, desolneux, richard}@math-info.univ-paris5.fr

Abstract. Usually, image registration and abnormality detection (e.g. lesions) in mammography are solved separately, although the solutions of these problems are strongly dependent. In this paper, we introduce a Bayesian approach to simultaneously register images and detect abnormalities. The key idea is to assume that pixels can be divided into two classes: normal tissue and abnormalities. We define the registration constraints as a mixture of two distributions which describe statistically image gray-level variations for both pixel classes. These mixture distributions are weighted by a map giving probabilities of abnormalities to be present at each pixel position. Using the Maximum A Posteriori, we estimate the deformation and the abnormality map at the same time. We show some experiments which illustrate the performance of this method in comparison to some previous techniques.

1 Introduction

Mammograms are often interpreted by comparing left and right breasts or successive mammograms of a same patient. Such comparisons help radiologists to locate suspicious differences which indicate the presence of some abnormalities [1]. Several Computer-Aided Diagnosis (CAD) systems have also used image comparisons for detecting abnormalities [2,3,4].

In these systems, a difference image is used to compare two images. This difference image is obtained by simple subtraction [2], weighted subtraction [3] or nonlinear subtraction [4]. Then it is thresholded to extract suspicious regions. However, the image comparison is not straightforward due to additional image dissimilarities which are related to sensor noise, different radiation exposure, and variation of breast positioning and compression and which cause high false-negative rates in abnormality detection schemes. Image registration is commonly carried out to compensate for these normal differences. Hence, the success of the detection task based on image difference depends on the preliminary registration process.

On the other hand, the registration problem is usually expressed as a minimization of an energy composed of a regularization term and a similarity term.

The definition of the similarity criterion relies on the nature of image gray-level dependencies [5]. For instance, the Sum of Square Differences (SSD) is often used whenever gray-level values are approximately the same in the two images to be registered. However, the presence of pathologies in mammograms such as lesions invalidates gray-level dependency assumptions. Hence, abnormalities may distort registration constraints and cause registration errors. Incorporating some knowledge about abnormalities can improve the registration.

In [6], F. Richard proposed a registration technique which down-weights the influence of abnormalities in the computation of registration constraints. The similarity criterion used is related to M-estimation criteria, also applied for optical flow computation [7]. But, the M-estimation approaches characterize abnormalities as pixels generating large image differences, which is not always the case. A more general approach consists of using mixture-based models, in which abnormalities are represented by a probability distribution, as it was done for the optical flow estimation by Jepson and Black [8], and for image registration by Hasler et al. [9], and by Hachama et al. [10].

In this paper, we present a mixture-based technique related to these previous works. The main feature of our model is the definition of a probability lesion map, which weights the mixture distributions at each pixel position by a probability to belong to a lesion. In this manner, we can interleave the registration and abnormality detection and thus take proper advantage of the dependence between the two processes.

The mixture-based technique and its mathematical formulation are presented in Section 2. In Section 3, we illustrate the method behavior on some examples and compare it with some classical techniques.

2 The Mixture-Based Technique

Let I and J be two images of the same size (M, N) , having gray-level values in the set $\{0, \dots, 255\}$ and defined on a discrete grid $\Omega_d = \{(\frac{i}{M-1}, \frac{j}{N-1}), (i, j) \in \{0, \dots, M-1\} \times \{0, \dots, N-1\}\}$ associated to $\Omega = [0, 1]^2$. Image coordinates are matched using applications ϕ which map Ω_d into itself. Usually, registering the source image I and the target image J consists of finding an application ϕ which is such that the deformed image $I_\phi = I \circ \phi$ is “similar” to the target image J .

We assume that lesions may be present in the images. Let L be the lesion map which associates to each pixel of Ω_d its probability to belong to a lesion. In the following, we formulate a bayesian model which allows us to estimate simultaneously the deformation ϕ and the lesion map L . Thus, we can solve the problems of image registration and abnormality detection at the same time.

2.1 Bayesian Formulation

Our formulation follows the Bayesian framework for image analysis laid out in [11]. Assuming that images, transformations and lesion maps are realizations of some random fields, Bayes rule can be expressed as

$$p(\phi, L|I, J) = \frac{p(I, J|\phi, L)p(\phi, L)}{p(I, J)}.$$

The Bayes rule allows us to write the posterior distribution $p(\phi, L|I, J)$ which contains the information about the unknowns ϕ and L , in terms of the prior $p(\phi, L)$ and the likelihood $p(I, J|\phi, L)$. The prior contains information about the most likely deformations and possible forms of lesions, namely, their morphology and spatial configuration. The relation between registered images is encapsulated in the likelihood term. The probability $p(I, J)$ is constant because it only depends on the observed fields I and J .

As a simplification, we assume that the deformation ϕ and the lesion map L are independent. In fact, lesions could generate specific local deformations that we choose to neglect. Thus, the Bayes rule can be written as

$$p(\phi, L|I, J) \propto p(I, J|\phi, L)p(\phi)p(L).$$

We can estimate the pair (ϕ, L) as the solution of the Maximum A Posteriori:

$$(\tilde{\phi}, \tilde{L}) = \arg \max_{(\phi, L)} p(I, J|\phi, L)p(\phi)p(L). \quad (1)$$

To ensure that the transformations remain smooth, we assume that they arise from the Gibbs distribution:

$$p(\phi) = \frac{1}{Z_1} e^{-H_d(\phi)}, \quad (2)$$

where Z_1 is a normalization constant, and H_d is a discrete elasticity potential [12] (a continuous version is given by Equation (9)). We also assume that the lesion map arises from a Gibbs distribution:

$$p(L) = \frac{1}{Z_2} e^{-R_d(L)}, \quad (3)$$

where Z_2 is a normalization constant, and R_d is a discrete energy of regularization. We use in this paper an energy restricting the amount of abnormal pixels in the images via a real parameter α_L :

$$R_d(L) = \alpha_L \sum_{x \in \Omega_d} L(x).$$

More specific terms can be defined to describe the spatial configurations of each type of lesion. We will investigate the use of such energies in the future.

In order to define the likelihood $p(I, J|\phi, L)$, we assume that, given the transformation ϕ , the probability of the pair of images (I, J) depends only on the registered images (I_ϕ, J) and that pixels are independent. Hence, we can write

$$p(I, J|\phi, L) = \prod_x p(I_\phi(x), J(x)|L(x)). \quad (4)$$

The probability of the pair $(I_\phi(x), J(x))$ depends on the class of the pixel x . Each class is characterized by a probability distribution, denoted by p_N for the normal tissue and p_L for the lesion. Thus, the probability distribution $p(I_\phi(x), J(x)|L(x))$ can be defined as a mixture of the two class distributions:

$$p(I_\phi(x), J(x)|L(x)) = (1 - L(x))p_N(I_\phi(x), J(x)) + L(x)p_L(I_\phi(x), J(x)). \quad (5)$$

The value of the lesion map L at location x is used to weight both class distributions. In what follows, we present the distributions p_N and p_L we used in experiments.

The Normal Tissue Class. Normally, gray-level values of registered images should be exactly the same at corresponding positions. But, in practice, these gray-level values usually differ because of noise or different image acquisition parameters. Assuming that these variations have a discrete Gaussian distribution with mean 0 and variance σ^2 ($\sigma = 15$ in the experiments), we can define p_N as

$$p_N(I_\phi(x), J(x)) = \frac{1}{C_1} \exp\left(-\frac{|I_\phi(x) - J(x)|^2}{2\sigma^2}\right), \quad (6)$$

where C_1 is the normalization constant.

The Lesion Class. The definition of the lesion distribution is a difficult task. Each type of lesion requires the definition of a specific distribution. For the sake of simplicity, we assume that a lesion is present in the target image J . We characterize the lesion just as an area which is brighter in the target image than it is in the source image, defining the following distribution:

$$p_L(I_\phi(x), J(x)) = \begin{cases} 0, & \text{if } I_\phi(x) > J(x) \\ \frac{1}{C_2}, & \text{otherwise,} \end{cases} \quad (7)$$

where C_2 is the normalization constant.

2.2 Numerical Resolution

Up to now, we have formulated a Bayesian registration model in a discrete setting. We now transform the discrete model into a continuous model so as to be able to use variational resolution techniques. First, we rewrite the MAP estimate (Equation (1)) as the minimization of the negative-log function

$$E_d(\phi, L) = -\log(p(\phi)) - \log(p(L)) - \log(p(I, J|\phi, L)).$$

Then, using Equation (4) and Gibbs distributions (2) and (3), we get

$$E_d(\phi, L) = H_d(\phi) + R_d(L) - \sum_{x \in \Omega_d} \log(p(I_\phi(x), J(x)|L(x))) + K,$$

where K is a constant. Next, following approaches in [13,12], we define a continuous expression of this energy, by interpolating all functions by the finite element method and replacing sums on the pixel grid Ω_d by integrals on Ω :

$$E(\phi, L) = H(\phi) + R(L) - \int_{\Omega} \log(p(I_{\phi}(x), J(x))) dx, \quad (8)$$

where the probability distribution $p(I_{\phi}(x), J(x))$ is the obtained continuous version of the mixture distribution given by Equation (5). $H(\phi)$ is the elasticity potential defined as

$$\sum_{i,j=1,2} \int_{\Omega} [\lambda \frac{\partial u_i(x)}{\partial x_i} \frac{\partial u_j(x)}{\partial x_j} + \mu (\frac{\partial u_i(x)}{\partial x_j} + \frac{\partial u_j(x)}{\partial x_i})^2] dx, \quad (9)$$

where $u = \phi - id$, and λ and μ are the Lamé elasticity constants. The term $R(L)$ is the following energy:

$$R(L) = \alpha_L \int_{\Omega} L(x) dx.$$

As in [14,6], we use a gradient descent algorithm on the energy E and finite elements to approximate solutions of the minimization problem. We use a variable change $L = \frac{1}{1+e^{-M}}$ so as to satisfy the constraints $0 \leq L(x) \leq 1$ and to be able to differentiate the energy with respect to the second variable M .

3 Results

In this section, we illustrate the characteristics of the mixture model by comparing its performance to those of the SSD technique [12], and the M-estimator based technique proposed in [6]. We applied algorithms to a pair of bilateral mammograms (case 21 of the MIAS database [15]), for which the target image contains a lesion (bright circular region at the bottom of Image (1-b)).

Registration results. Registrations obtained with the SSD and M-estimation techniques tend to incorrectly match the lesion and the bright tissue in the source image and thus reduce image differences due to the lesion (Images (1-d) and (1-e)). This is corrected by the mixture-based technique which registers the images correctly while preserving differences due to the lesion (Image (1-f)).

Detection results. We compare lesion binary images obtained with the three techniques. For the SSD and the M-estimation techniques, lesion binary images are obtained by thresholding the image difference generated by the adaptively weighted subtraction [3]. The fact that abnormal pixels tend to have relatively higher gray-level values is used to weight the difference between a pair of pixels by gray-level value of the pixel of the image J . For the mixture-based method, we set $\alpha_L = 0.1$ and threshold the lesion map. The thresholds are chosen so as to have the same amount of abnormal pixels in the three lesion binary images obtained. Figure 2 shows the lesion binary images obtained with the three techniques for different amounts of abnormal pixels.

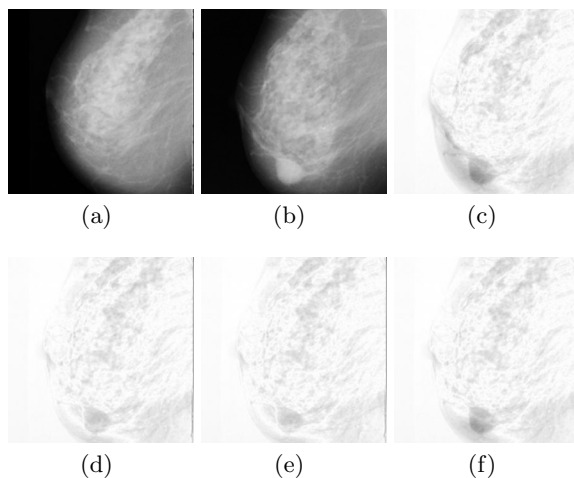


Fig. 1. Registration of bilateral mammograms. (a) Source image I, (b) Target image J, (c) The difference between the images before registration. The difference between the images after the registration using (d) the SSD method, (e) the M-estimation method, (f) the mixture-based method.

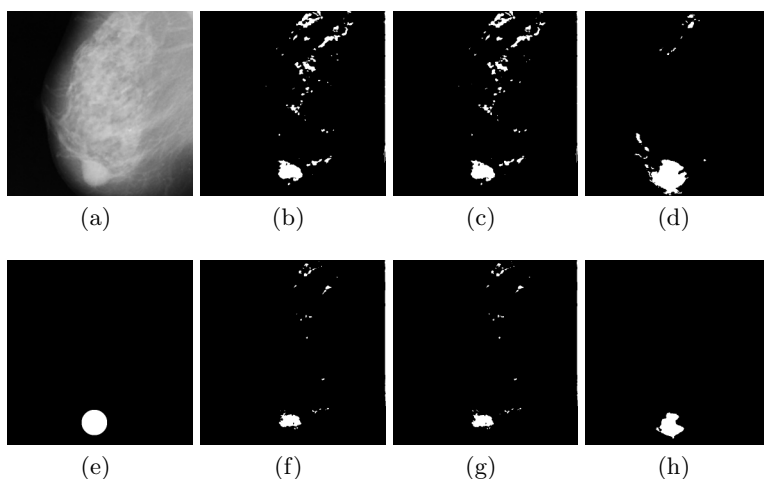


Fig. 2. The detection results. (a) The target image containing the lesion. For 10550 abnormal pixels, the results obtained with the (b) SSD method, (c) M-estimation based method, (d) The mixture-based method. (e) The expert segmented lesion. For 4180 pixels, the results obtained with the (f) SSD method, (g) M-estimation based method, (h) The mixture based method.

For evaluating and comparing the three algorithms without the influence of a threshold value, we have represented on Figure 3 the FROC curves obtained with the three methods. The FROC curve plots the sensitivity (fraction of detected true positives calculated by using the expert segmented image) as a function of the number of false positives. For the mixture-based technique, we have obtained similar FROC curves for different values of the weight α_L . We have represented the FROC curve obtained when $\alpha_L = 0.1$.

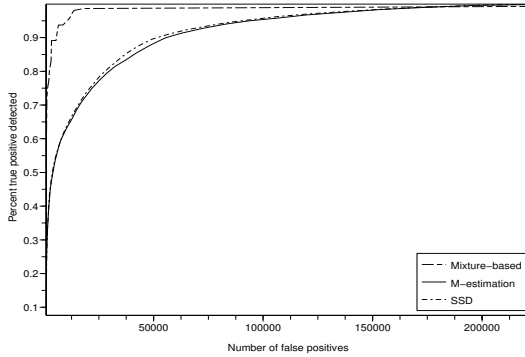


Fig. 3. FROC Curves for the three detection methods

As observed on Figure (3), the FROC curve associated to the mixture-based method is the highest. So, the detection by the mixture-based technique is more sensitive. For instance, for 10000 false positive pixels (2% of image pixels), the detection rate grows from 0.632 for the SSD and 0.627 for the M-estimation based method, to 0.947 for the mixture based method.

4 Conclusion

We have presented a method for joint mammogram registration and abnormality detection. Thanks to this combined approach, the mixture-based method improves the mammogram registration and increase the sensitivity of lesion detection. In the future, we will focus on how to design a lesion model for different types of lesions, and on the estimation of the distribution parameters for both lesion and normal tissue classes. Furthermore, we plan to apply the mixture method to a full mammogram database.

Acknowledgments. This work was supported by the grant “ACI Young Researchers 2003 (French Ministry of Research)” No. 9060.

References

1. L. Tabar and P. Dean, *Teaching atlas of mammography*, Thieme Inc., Stuttgart, 1985.
2. M. Sallam, G. Hubiak, K. Bowyer, and L. Clarke, "Screening mammogram images for abnormalities developing over time," in *IEEE Nuclear Science Symposium and Medical Image Conference*, 1992, pp. 1270–1272.
3. M.Y. Sallam and K. Bowyer, "Registration and difference analysis of corresponding mammogram images," *Medical Image Analysis*, vol. 3, no. 2, pp. 103–118, 1999.
4. F.F. Yin, M.L. Giger, K. Doi, C.E. Metz, C.J. Vyborny, and R.A. Schmidt, "Computerized detection of masses in digital mammograms: Analysis of bilateral-subtraction images," *Medical Physics*, vol. 18, pp. 995–963, 1991.
5. A. Roche, G. Malandain, and N. Ayache, "Unifying Maximum Likelihood Approaches in Medical Image Registration," *International Journal of Computer Vision of Imaging Systems and Technology*, vol. 11, pp. 71–80, 2000.
6. F. Richard, "A new approach for the registration of images with inconsistent differences," in *Proc. of the Int. Conf. on Pattern Recognition, ICPR*, Cambridge, UK, 2004, vol. 4, pp. 649–652.
7. N. Sebe and M.S. Lew, *Robust Computer Vision: Theory and Applications*, vol. 26, Series: Computational Imaging and Vision, 2003.
8. A. Jepson and M.J. Black, "Mixture models for optical flow computation," in *IEEE Conf. on Computer Vision and Pattern Recognition*, 1993, pp. 760–761.
9. D. Hasler, L. Sbaiz, S. Susstrunk, and M. Vetterli, "Outlier modeling in image matching," *IEEE Trans. on Patt. Anal. and Match. Intell.*, pp. 301–315, 2003.
10. M. Hachama, F. Richard, and A. Desolneux, "A mammogram registration technique dealing with outliers," *University Paris 5, MAP5 Technical Report*, www.math-info.univ-paris5.fr/map5/publis/, January 2006.
11. D. Mumford, "The bayesian rationale for energy functionals," *Geometry-driven Diffusion in Comp. Vis.*, *Kluwer Academic Publ*, vol. 46, pp. 141–153, 1994.
12. F. Richard, "A comparative study of markovian and variational image-matching techniques in application to mammograms," *Pattern Recognition Letters*, vol. 26, no. 12, pp. 1819–1829, 2005.
13. M.I. Miller, G. Christensen, Y. Amit, and U. Grenander, "Mathematical textbook of deformable neuroanatomies," in *Proc. Natl. Acad. Sc.*, USA, 1993, pp. 11944–11948.
14. F. Richard and L. Cohen, "Non-rigid image registration with free boundary constraints: application to mammography," *Journal of Computer Vision and Image Understanding*, vol. 89(2), pp. 166–196, 2003.
15. J. Suckling, J. Parker, and D. Dance, "The MIAS digital mammogram database," *In Proc. of the 2nd Int. Workshop on Digital Mammography, England*, July 1994.